Research on Dragon Dance Formation Modeling and Collision Detection Based on Spiral Motion Model

Hanting Di [1,*], Jiayi Mo [2]

[1] Portland Institute, Nanjing University of Posts and Telecommunications, Nanjing, China, 210023

[2] College of Internet of things, Nanjing University of Posts and Telecommunications, Nanjing, China, 210023

* Corresponding Author Email: p22000404@njupt.edu.cn

Abstract. In dragon dance performances, precise control of formations and collision avoidance are crucial for enhancing performance quality and safety. In recent years, mathematical modeling and computational algorithms have become key research directions for optimizing dragon dance formations. This study proposes a modeling approach based on the Archimedean spiral to analyze the dynamic behavior of the "bench dragon" (a specific type of dragon in the formation) along complex paths. By numerically solving the differential equations and geometric constraints using the forward Euler method, the spatial distribution of the segments of the "bench dragon" is obtained, and its dynamic evolution is simulated through time-stepping discretization. The results indicate that the distance between the "bench dragon" and the origin gradually decreases. Within the first 300 seconds, the distance of the dragon head decreases by 3.8027 meters, and that of the dragon tail decreases by 2.4486 meters, with more significant changes occurring in the segments closer to the head. To prevent collisions, the minimum safe distance between the segments is maintained above 0.8 meters, and the maximum position deviation between the dragon head and tail is reduced to 1.3%. However, the inward spiral contraction characteristic of the Archimedean spiral may increase the risk of trajectory overlap or collision in the central region of the spiral. This study provides significant theoretical support and practical reference for the dynamic optimization of multi-segment flexible systems.

Keywords: Archimedes Spiral, Forward Euler Method, Polar Trajectory Optimization, Velocity Correlation Analysis, Multi-node Connected Rigid Body Dynamics.

1. Introduction

Dragon dance, as one of the symbols of Chinese traditional culture, not only carries rich historical and cultural connotations but is also an important part of folk celebrations and festive activities [1]. For the bench dragon, ensuring smooth performance progression requires precise formation control and collision avoidance, which have become critical issues to address. In traditional bench dragon performances, collisions and misalignments between the benches are common, which can negatively impact the overall performance and safety. Therefore, optimizing the movement path of the formation through scientific methods and effectively avoiding collisions between the benches is key to improving performance quality and safety. In recent years, with the development of motion modeling and computer simulation technologies, the use of mathematical modeling and computational algorithms to optimize dragon dance formations has become a new research trend.

This study focuses on the dynamic behavior of the bench dragon moving along an Archimedean spiral at a constant speed. By analyzing and simulating the position distribution of each bench at different times, the study explores the movement of the formation. First, the movement trajectory of the dragon head's front handle is defined based on the Archimedean spiral, and the dynamic trajectory is obtained by numerically solving the differential equations, which lack explicit solutions, using the forward Euler method. Then, by applying geometric constraints with a fixed distance between each handle, coordinate transformation is used to derive the position information of adjacent handles, thus calculating the spatial distribution of the entire dragon. To ensure the movement conforms to actual physical laws, the study further establishes a velocity transfer relationship between the dragon head and the segments of the dragon body and uses time-stepping discretization methods to simulate the dynamic evolution of the entire dragon. Finally, an in-depth analysis is conducted on the movement deviations caused by path contraction and velocity differences, exploring their potential impacts on system stability and movement consistency.

The marginal contribution of this study lies in its development of a novel dynamic modeling approach combining Archimedean spiral trajectories and forward Euler numerical methods to address the gap in precise trajectory optimization for bench dragon performances. By introducing a velocity transfer relationship and dynamic discretization framework, the study enables realistic simulation of inter-segment motion coordination and effective collision avoidance, while also offering a practical foundation for applying these optimization techniques to broader fields such as robotics and biomechanics. These advancements enhance both the theoretical understanding and practical implementation of multi-segment flexible systems [2, 3].

2. Motion Analysis of Dragon Dance Formation on Spiral Path

2.1. Overview of the Dragon Dance Structure

Given a bench dragon consisting of one dragon head, 221 dragon body segments, and one dragon tail, all bench widths are identical. The lengths of the dragon body and dragon tail segments are the same, and adjacent benches are connected via handrails. The connection between the dragon head and the first body segment, along with the corresponding dimensions and data, is shown in Figure 1.

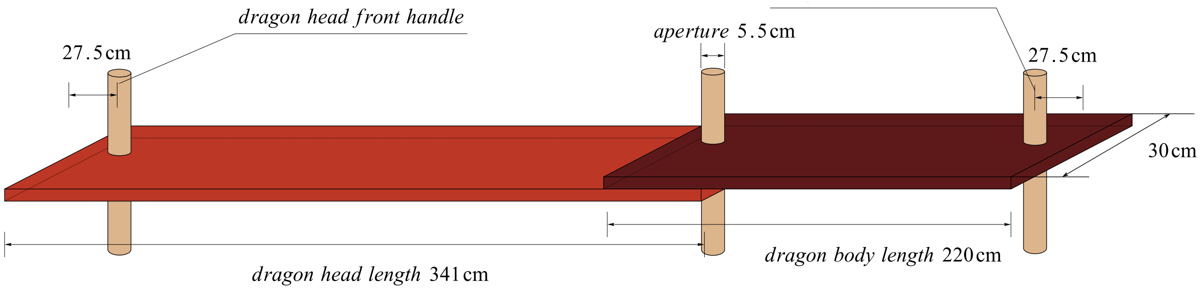

Figure 1. Schematic diagram of bench connection

2.2. Archimedean Spiral Path

The coiled path is an equidistant spiral with a pitch of 55 cm. Initially, the dragon head is located at point A on the 16th turn of the spiral. The forward velocity remains constant at 1 m/s, and the centers of all handrails lie on the spiral, meaning the trajectory of each handrail follows the equidistant spiral shown in Figure 2. Here, A represents the initial position of the dragon head.

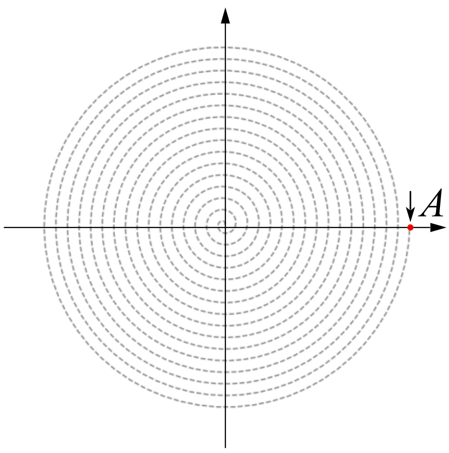

Figure 2. Isometric spiral diagram of handle trajectories

An equidistant spiral, also known as an Archimedean spiral, is a trajectory generated by a point moving away from a fixed center at a uniform speed while rotating around the center at a constant angular velocity [4-6]. For such a curve, its polar coordinate equation offers a more convenient expression for analysis. Therefore, the specific equation of the spiral where the handrail trajectories lie is given as:

$$r = a + b\theta \tag{1}$$

Where r is the radial distance from the origin at angle θ, and b is the increment in radial length per unit increase in θ, controlling the pitch of the spiral. The pitch p is calculated as:

$$b = \frac{dr}{d\theta} = \frac{P}{2\pi} \tag{2}$$

2.3. Handle Movement and Velocity Decomposition

The bench dragon consists of multiple long benches connected sequentially at their front and rear handrails. Determining the positions of the handrails is a critical prerequisite for analyzing the relative velocities between adjacent benches. The front handrail of the dragon head starts at point A with a constant speed of 1 m/s. Its motion analysis is shown in Figure 3.

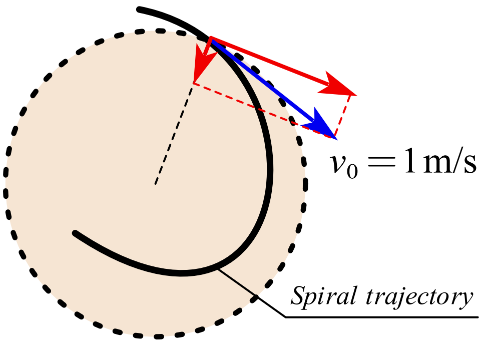

Figure 3. Faucet front handle motion analysis

According to the definition of the equidistant spiral, the front handrail of the dragon head moves along the spiral, combining uniform linear motion away from the center and uniform circular motion around the center. The resultant velocity v is tangential to the trajectory and directed clockwise, with a magnitude of 1 m/s [7, 8]. In polar coordinates, the resultant velocity v_o can be decomposed into radial velocity v_r and tangential velocity v_q as:

$$v_0^2 = v_r^2 + v_q^2 = \left(\frac{dr}{dt}\right)^2 + \left(r\frac{d\theta}{dt}\right)^2 \tag{3}$$

Combining Equation (3) and the expression for vr, we derive the following differential equation:

$$\frac{dr}{dt} = \frac{d}{dt}(a + b\theta) = b\frac{d\theta}{dt} \tag{4}$$

Simultaneous equations (3) and (4) are simplified to give the following differential equation:

$$\sqrt{b^2 + (a + b\theta)^2}\,d\theta = dt \tag{5}$$

There is no explicit solution to this differential equation and can only be solved by numerical solution, here by the pre-Eulerian method. For Eq. (5), through the discretization time, the differential equation is converted into a difference equation for recursion, the step size is set $h = 1s$, and the initial pole diameter θ_0 is the pole diameter corresponding to the starting point of the front handle of the faucet A, and the recursive formula is as follows:

$$\theta_{n+1} = \theta_n + hf\left(\theta_n, t_n\right) = \theta_n + h\frac{1}{\sqrt{b^2 + \left(a + b\theta\right)^2}} \tag{6}$$

Thus, at a given time, the polar coordinates of the front handle of the faucet are $\left(r\left(\theta\right), \theta\left(t\right)\right)$.

2.4. Adjacent handle Recursive Relationship

The center of the handle of each bench is coiled into the spiral, and the relative distance remains the same. Therefore, the connection of each handle to the previous hand can be regarded as a fixed length of moving secant on a spiral. The geometric relationship between the dragon head and the first dragon body is shown in Figure 4.

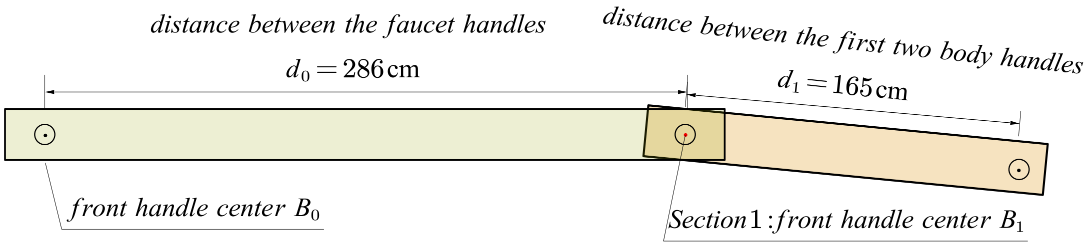

Figure 4. The geometric relationship between the head and the first section

In polar coordinates, the formula for coordinates $\left(r_a, \theta_a\right)$ and $\left(r_b, \theta_b\right)$ distances are:

$$L = \sqrt{r_a^2 + r_b^2 - 2r_a r_b \cos\left(\theta_a - \theta_b\right)} \tag{7}$$

Substituting the center of the front handle of the first section of the dragon body $B_1\left(r_1, \theta_1\right)$ and the center of the front handle of the dragon head $B_0\left(r_0, \theta_0\right)$,

$$d_0 = \sqrt{\left(a + b\theta_0\right)^2 + \left(a + b\theta_1\right)^2 - 2\left(a + b\theta_0\right)\left(a + b\theta_1\right)\cos\left(\theta_1 - \theta_0\right)} \tag{8}$$

Among them, the distance between the dragon head handlebars, and the right limit $\theta_1 - \theta_0$ ensures that the correct center of the first section of the dragon body front handle is found at many points on the spiral line that meet the distance requirements. From this formula, we can obtain the polar angle θ_1 corresponding to the center of the front handle of the first dragon body.

2.5. Comprehensive Solution of Position and Velocity

The speed of the front handle of the faucet is constant and known, and the planks do not deform during travel. Therefore, the velocity of the rear grip (i.e., the next section of the front handle) can be obtained about the speed of the front handle [9, 10].

According to the analysis of the speed direction of the front handle of the faucet, it can be known that the speed direction of each handle is the clockwise tangent direction of the point on the spiral. Through the parametric equation of Eq. (3), the velocity direction of the handle in the Cartesian coordinate system is obtained by deriving. Taking the ith dragon body handle as an example, the velocity direction vector n_i is:

$$\overrightarrow{n_i} = \left(b\cos\theta_i - \left(a + b\theta_i\right)\sin\theta_i, b\sin\theta_i + \left(a + b\theta_i\right)\cos\theta_i\right) \tag{9}$$

As shown in Figure 5, taking the faucet as an example, the front handle, the rear handle, and its connecting part are simplified into a rod, and the rod cannot be stretched or compressed because the wooden board does not deform during the march. The speed of the front and rear handles is the same along the direction of the rod, and the speed is correlated, that is $v_0 \cos\alpha_0 = v_1 \cos\alpha_1$. Wherein,

v_0 is the speed of the front handle of the faucet, v_1 is the speed of the rear handle of the faucet (i.e., the front handle of the first section of the dragon body), α_0 is the angle between the speed of the front handle of the faucet and the direction of the rod, and α_1 is the angle between the speed of the rear handle of the faucet and the direction of the rod.

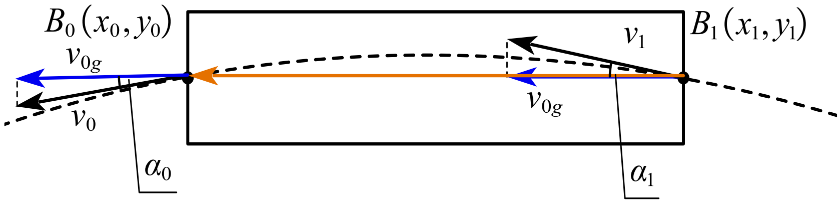

Figure 5. Schematic diagram of faucet speed correlation

$$\begin{cases} \overrightarrow{n_i} = \left(b\cos\theta_i - (a+b\theta_i)\sin\theta_i, b\sin\theta_i + (a+b\theta_i)\cos\theta_i\right) \\ \overrightarrow{n_{i-1}} = \left(b\cos\theta_{i-1} - (a+b\theta_{i-1})\sin\theta_{i\text{-}1}, b\sin\theta_{i\text{-}1} + (a+b\theta_{i\text{-}1})\cos\theta_{i\text{-}1}\right) \\ \cos\alpha_i = \dfrac{\overrightarrow{n_i} \cdot \overrightarrow{B_iB_{i-1}}}{\left|\overrightarrow{n_i}\right|\left|\overrightarrow{B_iB_{i-1}}\right|} \\ \cos\alpha_{i-1} = \dfrac{\overrightarrow{n_{i-1}} \cdot \overrightarrow{B_iB_{i-1}}}{\left|\overrightarrow{n_{i-1}}\right|\left|\overrightarrow{B_iB_{i-1}}\right|} \\ B_iB_{i-1} = \left((a+b\theta_i)\cos\theta_i - (a+b\theta_{i-1})\cos\theta_{i-1}, (a+b\theta_i)\sin\theta_i - (a+b\theta_{i-1})\sin\theta_{i-1}\right) \end{cases} \tag{10}$$

Among them, θ_i is the size of the polar angle of the center of the front handle of the ith dragon in polar coordinates.

3. Handle Trajectory and Velocity Results

3.1. Handle Trajectory Simulation

The spiral departs from the origin, and the distance is zero when $\theta = 0$ to the origin, that is $a = 0$. Knowing the pitch $P = 0.55\text{m}$, brought in equation (2), the solution $b = 0.55/2\pi$ obtains that the spiral equation where the handle trajectory is located is:

$$r = \frac{0.55}{2\pi}\theta \tag{11}$$

Taking the center of the front handle of the dragon head and the center of the front handle of the first section of the dragon body as examples, the path within 0~300s is simulated in Figure 6.

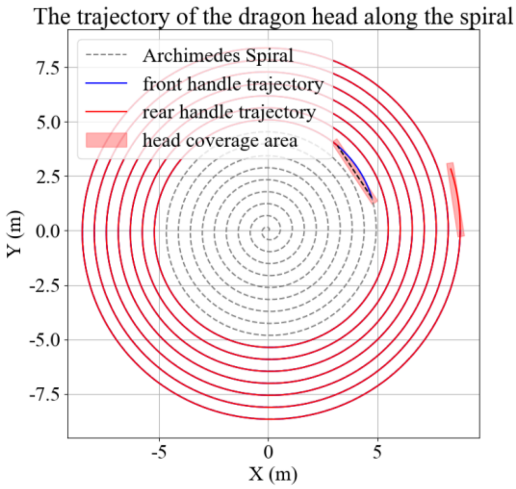

(a) Movement process of the faucet bench

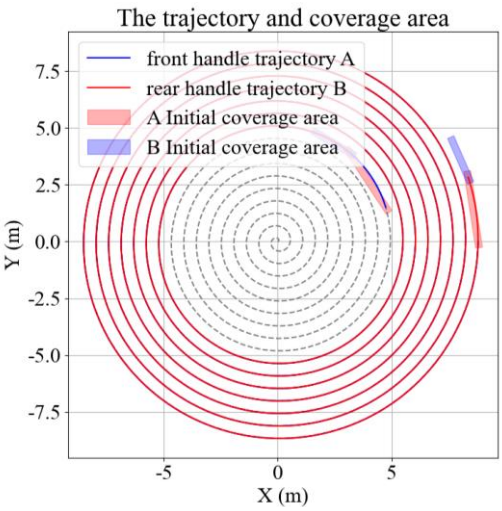

(b) The movement process of the dragon body bench in the first section

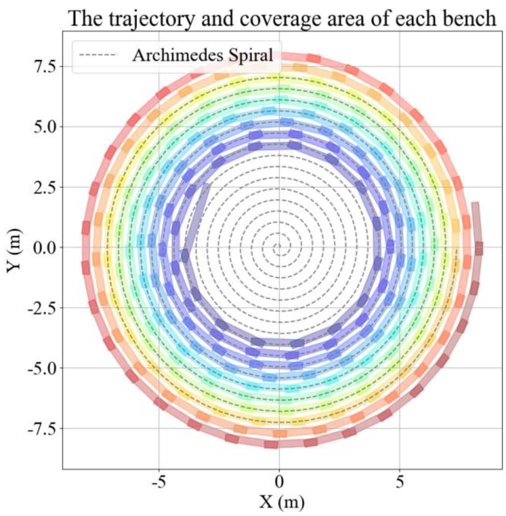

(c) Schematic diagram of the state of the bench dragon when t=300s

Figure 6. Schematic diagram of the path within 0~300s

As can be seen from Figure 6 (a) (b), the trajectories of the center of the front handle of the dragon head and the front handle of the first section of the dragon body follow the spiral equation, and the distance remains constant. Similarly, the coordinates of 224 handles per second in 0~300s are calculated, and the results are shown in Table 1.

Table 1. Results of each bench position

	0s	60s	120s	180s	240s	300s
Faucet x(m)	8.80000	5.82510	-4.01887	3.08103	2.76991	4.28626
Faucet y(m)	0.00000	5.74552	-6.34785	6.03816	5.27142	2.56917
1st Body x(m)	8.36382	7.47228	-1.36805	5.32084	4.93686	2.21144
1st Body y(m)	2.82654	3.40749	-7.42151	4.25972	3.40489	4.53760
51st Body x(m)	9.51873	8.69680	-5.60304	2.76959	6.08484	6.31976
51st Body y(m)	1.34114	2.50527	6.32649	7.29789	3.66349	0.18442
101st Body x(m)	2.91398	5.71691	5.42655	2.02594	4.76296	6.38638
101st Body y(m)	9.918312	7.98052	-7.51230	8.44346	6.49859	3.69660
151st Body x(m)	10.86173	6.65437	2.312210	0.87573	2.78171	6.89010
151st Body y(m)	1.82875	8.15781	9.74660	9.43886	8.46434	4.63103
201st Body x(m)	4.55510	6.64912	10.63758	9.23385	7.33278	7.29496
201st Body y(m)	10.72512	9.00425	1.28163	4.36518	6.33048	5.49252
Tail x(m)	-5.30544	7.39258	10.96865	7.29138	3.05683	1.50821
Tail y(m)	10.67658	8.77482	0.92217	7.58394	9.53219	9.35268

The distance between the bench dragon and the origin decreases over time as the bench dragon moves towards the origin as a whole. Specifically, the distance between the front handles of the dragon's head, body, and tail and the origin shows different rates of change. The most pronounced change in the distance between the dragon's head and the origin, which decreased by 3.8027 meters in the first 300 seconds, showing a significant reduction in distance, compared to the slower change in the distance between the dragon's tail and the origin, which decreased by only 2.4486 meters in the first 300 seconds. Overall, the closer you get to the faucet, the more significant the change in the distance between the front handle and the origin.

During the movement of the bench dragon, the dragon head did not significantly collide with other parts in the time range from 0 to 300 seconds. As can be seen from the position map, the positions of the individual front and rear handles and benches are maintained at a high distance from other benches, so it can be assumed that there were no overlaps or collisions during this period.

However, when the Bench Dragon traveled along the spiral path, the inward contraction of the spiral caused the Bench Dragon to gradually decrease from the center of the spiral. Over time, this trend may increase the risk of overlapping or colliding parts of the bench dragon, especially in areas closer to the center of the spiral.

3.2. Handle Velocity Simulation

The obtained coordinates at each time and the coiled spiral equation are brought into Eq. (9), and the parameters such as the velocity direction vector and the plate direction vector of each handle at each time are obtained by Python programming, and the velocity is obtained by correlating the velocity, and the result is shown in Table 2.

Table 2. Partial velocity results

	0s	60s	120s	180s	240s	300s
Faucet (m/s)	1.000000	1.000000	1.000000	1.000000	1.000000	1.000000
1st Body (m/s)	0.999971	0.999961	0.999945	0.999917	0.999859	0.999711
51st Body (m/s)	0.999741	0.999662	0.999538	0.999331	0.998943	0.99807
101st Body (m/s)	0.999575	0.999453	0.999269	0.998972	0.998438	0.997310
151st Body (m/s)	0.999448	0.999299	0.999078	0.998728	0.998117	0.996870
201st Body (m/s)	0.999348	0.999180	0.998935	0.998552	0.997896	0.996584
Tail (m/s)	0.999311	0.999137	0.998883	0.998490	0.997819	0.996487

The speed of the front handle of the bench dragon shows a certain regularity with time, and the speed of the front handle of the dragon head is always kept constant, at 1 m/s, which is not affected by time change. In contrast, the speed of the front handle and the rear handle of the dragon gradually decreases with time, and on the whole, the speed of the bench dragon shows a decreasing trend with time.

In terms of the difference in speed change, the speed of the front handle of the dragon head is always stable, while the speed of the front handle of the dragon body and the rear handle of the dragon tail decreases significantly. Especially for the dragon body, the farther away from the dragon head, the more significant the speed change of the handle, which indicates that the speed change of the bench dragon at different positions has a certain non-uniformity.

From the perspective of risk, since the speed of the dragon head is always maintained at 1 m/s, which is significantly higher than the speed of the dragon body and tail when the time exceeds 300 seconds, the dragon head gradually enters the inner circle of the spiral path. At this time, the joints of the dragon's body and tail may be difficult to keep up with the trajectory of the dragon's head due to the difference in speed, which increases the risk of overlapping trajectories or collisions.

4. Conclusion

This study drew several key conclusions from the movement analysis of the dragon dance formation. In terms of position, the distance between the front handle and the origin of the faucet gradually decreases from 8.8 meters to 4.29 meters in 0 to 300 seconds. In terms of speed, the speed of the faucet is always maintained at 1m/s, while the speed of the other benches gradually decreases. Further analysis of the handle position showed that the distance between the front handle of the dragon's head, the dragon's body, and the dragon's tail gradually decreased, and the distance between the dragon's head and the origin changed the most drastically, with a change of 3.80 meters in the first 300 seconds, while the distance between the dragon's tail and the origin changed slightly, only 2.45 meters.

The motion analysis framework proposed in this paper provides valuable ideas for research in related fields. The method combines path modeling, velocity decomposition, and numerical simulation to verify its feasibility and effectiveness in dynamic system analysis. This framework is not only applicable to the study of dragon dance formations, but also to a wide range of fields such as robotics, biomechanics, and other dynamic system analyses involving multiple interacting motion component.

However, the path modeling does not fully account for errors in complex scenarios, and the velocity model excludes external environmental factors. Future work will focus on incorporating more sophisticated modeling methods and considering various environmental variables. Additionally, the method's applicability will be extended to scenarios such as motion analysis on non-planar terrains or dynamic systems like bionic robots and multi-joint manipulators. These improvements will further enhance the theoretical value and practical applicability of this research.

References

[1] S. X, P. W H, C. L, et al. Drunken Dragon Cyber Dance: Application of Augmented Reality Technology in Drunken Dragon Cultural Heritage Education [C]//. 2022 2nd International Conference on Social Sciences and Intelligence Management (SSIM), 2022: 36 - 40.

[2] WANG X, CARPENTER H J, GHAYESH M H, et al. A review on the biomechanical behaviour of the aorta [J]. Journal of the Mechanical Behavior of Biomedical Materials, 2023, 144: 105922.

[3] SI J, THELKAR A R. Leveraging artificial neural networks for enhanced athlete performance evaluation through IMU data analysis [J]. Heliyon, 2024, 10 (15): e34826.

[4] H. C, CHENG Y. Approximation of Archimedes spiral with polynomial s-power basis [C]//. 2011 3rd International Conference on Computer Research and Development, 2011: 249 - 251.

[5] C. O, J. M M, K. T C, et al. Development of a Dual Wind Turbines using the Savonius and Archimedes Spiral Principle [C]//. 2018 IEEE 10th International Conference on Humanoid, Nanotechnology, Information Technology, Communication and Control, Environment and Management (HNICEM), 2018: 1 - 5.

[6] MAGEE R, YANG B, RATLIFF J. Trsper: a web-based application for Archimedes spiral analysis[J]. mHealth, 2022, 8: 3.

[7] T. K L, S. H B, S. Y O, et al. Complete coverage algorithm based on linked smooth spiral paths for mobile robots [C]//. 2010 11th International Conference on Control Automation Robotics & Vision, 2010: 609 - 614.

[8] C. E B, C. M D O, P. A, et al. GHASP: an Hα kinematic survey of spiral galaxies – X. Surface photometry, decompositions and the Tully–Fisher relation in the Rc band [J]. Monthly Notices of the Royal Astronomical Society, 2015, 453 (3): 2965 - 2981.

[9] H. W, J. Y, W. C. Methodologies on Spatial and Temporal Correlation Analysis between Regional Neighboring Sites[C]//. 2024 IEEE 19th Conference on Industrial Electronics and Applications (ICIEA), 2024: 1 - 4.

[10] S. R, T. W, L. J, et al. Research on equivalent modeling method of wind farm considering wind speed correlation based on Mixed-Copula [C]//. 2021 IEEE Sustainable Power and Energy Conference (iSPEC), 2021: 602 - 607.